ADVANCED MATERIALS TECHNOLOGIES
www.advmattechnol.de

Mitigating Water Crossover by Crosslinked Coating of Cation-Exchange Membranes for Brine Concentration

*Alexandra Rommerskirchen, Hannah Roth, Christian J. Linnartz, Franziska Egidi, Christian Kneppeck, Florian Roghmans, and Matthias Wessling**

Undesired water crossover through ion-exchange membranes is a significant limitation in electrically driven desalination processes. The effect of mitigating water crossover is twofold: 1) The desalination degree is less reduced due to the unwanted removal of water, and 2) the brine concentration is increased due to decreased dilution by an unwanted crossover of water molecules. Hence, water crossover limits the desalination and concentration efficiency of the processes, while the energy demand to achieve a certain level of desalination or concentration increases. This effect is especially pronounced when treating high salinity solutions, which goes hand in hand with the crossover of many ions through the ion-exchange membranes. A crosslinked coating for cation-exchange membranes (CEMs) is presented in this work, which can significantly mitigate such undesired water crossover. The efficacy is demonstrated using the flow-electrode capacitive deionization process applied for desalination and concentration of saline brines at feed concentrations of 60 and 120 g L^{-1} NaCl. With just a single coated CEM, the water crossover was reduced by up to 54%.

1. Introduction

Water is essential for life, as well as for many industrial processes. Significant research efforts are made for developing sustainable water treatment processes suitable for the desalination and concentration of aqueous streams.[1–3]

Electrically driven membrane processes applying ion-exchange membranes, such as electrodialysis (ED), membrane capacitive deionization, and flow-electrode capacitive deionization (FCDI), are promising candidates for challenging water desalination and brine concentration tasks.[4,5] However, undesired water crossover is a major limitation in such processes applying ion-exchange membranes. The effect is twofold: 1) the water stream, which is to be desalinated, is desalinated less efficiently due to the unwanted removal of water; and 2) the brine stream, which is to be concentrated, is concentrated less efficiently, due to the unwanted crossover of water molecules into the brine stream.[6,7] Hence, the desalination and concentration efficiency of the processes are limited, while the energy demand to achieve a certain level of desalination or concentration is increased. This effect is especially pronounced when treating high salinity solutions, which goes hand in hand with high concentration differences across the membranes and the crossover of a large number of ions including their hydration shells through the ion-exchange membranes.[8,9]

The issue of water crossover through proton exchange membranes is intensively studied and addressed in numerous publications.[10] Whereas, the mitigation of water crossover in cation-exchange membranes (CEM) is an overlooked domain in ion transport and high salinity conditions are rarely studied.

1.1. ED and FCDI Fundamentals

Electrodialysis (ED) and FCDI are electrical potential driven desalination techniques. The ions move in an electric field toward the oppositely charged electrode, respectively. Thus, ions are selectively separated from the water. Electrodialysis uses a stack of ion-exchange membranes creating separate diluate and concentrate channels. Faradaic reactions convert the applied electric current in the electrode chambers filled with a rinse solution.[11,12] The principles of ED have already been described in 1940, and the first commercial application of ED for brackish water treatment is known since the early 1950s. A further field of application for ED is the food industry, where ED can be used to produce table salt or for the deacidification of apple juice.[13]

Within the family of electrically driven desalination processes, FCDI is a novel technology, bearing promising potentials for the future of efficient water treatment. In 2013, Jeon et al., introduced FCDI, where static porous carbon electrodes from membrane capacitive deionization are replaced by carbon slurries, which allow for continuous desalination operation.[4,14,15]

Dr. A. Rommerskirchen, H. Roth, C. J. Linnartz, F. Egidi, C. Kneppeck, Prof. M. Wessling
DWI – Leibniz-Institute for Interactive Materials
Forckenbeckstraße 50, 52074 Aachen, Germany

Dr. A. Rommerskirchen, H. Roth, C. J. Linnartz, F. Egidi, C. Kneppeck, Dr. F. Roghmans, Prof. M. Wessling
Chemical Process Engineering AVT.CVT
RWTH Aachen University
Forckenbeckstraße 51, 52074 Aachen, Germany
E-mail: Manuscripts.cvt@avt.rwth-aachen.de

The ORCID identification number(s) for the author(s) of this article can be found under https://doi.org/10.1002/admt.202100202.

DOI: 10.1002/admt.202100202

In FCDI, a flow electrode is used instead of a rinse solution in the electrode chambers as in electrodialysis. The flow electrode consists of an electrolyte solution with suspended conductive particles, and the ions adsorb to the particles. Instead of faradaic reactions, the charge transfer happens through particle electrode interactions and capacitive ion storage.[5,16–18] With FCDI, a new variety of energy-efficient applications using selective desalination are demonstrated.[19,20]

1.2. Water Crossover in ED and FCDI Processes

In electrically driven desalination processes, the overall desalination and concentration performance are limited by back diffusion and undesired water crossover from diluate to concentrate.[7–9,21] The water crossover in such processes is mainly caused by osmotic and electro-osmotic water fluxes through the ion-exchange membranes. Different parameters can be influenced, such as the membrane thickness and various material characteristics.[22,23]

Achieving efficient salt removal with a high water recovery is challenging. Understanding the limiting factors is crucial for future improvements. Several studies exist, investigating the water transport between diluate and concentrate in ED.[7,21,24]

First results indicate that especially the treatment of highly saline brines[8] leads to increased osmotic and electro-osmotic water transfer rates in FCDI. The membrane material plays a vital role in influencing the water crossover in FCDI processes, which is the focus of this paper.

1.3. Nanofiltration and Nanofiltration Membranes

Nanofiltration is a pressure-driven membrane process used for ion retention. Typically, thin-film composite membranes are employed, consisting of a porous mechanically stable support and a thin dense separation layer coated on top.[25] Such separation layers evolve from interfacial polymerization.[26] The combination of the reactants piperazine and trimesoyl chloride (TMC) is a much studied material system and commercially applied in nanofiltration membranes.[27] The resulting polypiperazine-amide film has a negative charge and swells only slightly in water.[28] In nanofiltration application, water passes the membrane driven by the applied pressure which opposes the osmotic pressure. Ion transport in nanofiltration membranes is not yet fully understood.[29] Modeling approaches combine the effects Donnan exclusion, steric hindrance, and dielectric exclusion.[30] Especially, gaining more insight into the dielectric exclusion which includes the dehydration of ions when partitioning into the pore is strongly pursued.[29–33] Dehydration occurs when the hydrated ion is larger than the size of the pores.[34] In nanofiltration, either both anions and cations permeate or both are rejected to satisfy electroneutrality. Differences in free hydration energy contribute to the explanation of the selectivity for different salts. Sodium and chloride have low hydration energies[32] and it is assumed that sodium and chloride lose or at least partially lose their hydration shell before entering the pores of a polypiperazine-amide layer. This results in permeation of NaCl. Nanofiltration membranes are optimized for high divalent salt rejection while achieving high water permeation at elevated pressures.

In electrically driven processes, polyamide layers are rarely studied. So far applying an electric field as driving force was used for fundamental investigations to observe anion and cation transport separately.[29] Recently, commercial NF270 nanofiltration membranes have been employed in FCDI experiments. When replacing the anion exchange membrane in an FCDI setup with a nanofiltration membrane, monovalent selectivity of anions was achieved.[35] This is an indication that the dehydration of ions during ion transport is transferable to electrically driven processes. To the best of our knowledge, the dehydration of ions occurring during partitioning into the pore of polyamide layers and the low swelling of the material has not been exploited to decrease the water crossover in electrically driven desalination processes.

1.4. Ion Exchange Membranes

Ion exchange membrane consist of highly charged polymers.[36] The membranes are operated with an electric field as driving force via Donnan exclusion ions of the same charge as the membrane are retained while ions of opposite charge pass the charged polymer. Partitioning at the membrane surface is governed by the ion sorption into the charged polymer.[37] The charged groups in the membrane material are hydrated which means ion exchange membranes swell significantly in water. Ion exchange membranes are designed for the selective transport of either anions or cations while minimizing their resistance to the electrically driven process.

1.5. Modification of Ion Exchange Membranes

The successful surface coating and modification of ion exchange membranes have been reported for various purposes. Coating of ion exchange membranes with polyelectrolytes or surface modification via plasma treatment induced monovalent ion permselectivity. An overview of the coating techniques and materials is given in recent reviews.[36,38] The patterning of the surface of ion exchange membranes has shown to reduce the plateau length in electrodialysis.[39] Wang et al. show the double-sided coating of CEMs with piperazine and trimesoyl chloride, which induces monovalent selectivity.[40] However, reduced water crossover was not reported.

1.6. Concept: Crosslinked Membrane Coating for Mitigating Water Crossover

In this work, we present a crosslinked coating for CEMs. The concept is illustrated in **Figure 1** and aims at reducing the water crossover. A significant driver for the water crossover is electro-osmosis. Reducing the amount of water, which is transferred through the ion-exchange membranes together with the salt ions, would significantly reduce the overall water transfer. The membranes with a strongly crosslinked surface may retain the transfer of parts of the ions hydration shells in the diluate or

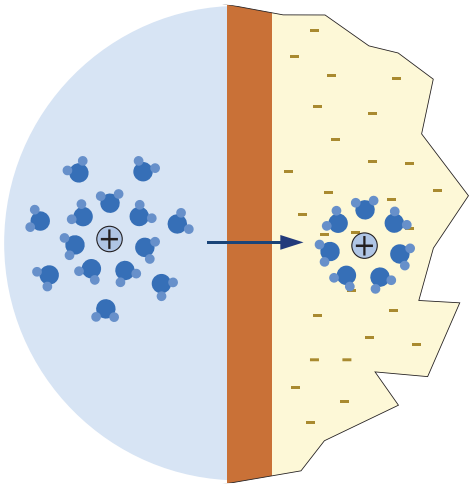

Figure 1. Illustration of the concept for a membrane with crosslinked surface for reducing the electro-osmotic water crossover in an ion-exchange membrane process.

concentrate channel. Additionally, the drag of water molecules in connection with the ion transfer and purely osmotic water passage might be reduced as well. By choosing a layer chemistry related to nano filtration, low additional resistance for ion transport is envisioned.

We have identified a new surface modification to suppress water crossover. The membranes are tested under high salinity conditions and the membrane is tested in a bench-scale process. We demonstrate the efficacy of the presented crosslinked coating at the example of a FCDI process applied for the desalination and concentration of saline brines at feed concentrations of 60 and 120 g L^{-1} NaCl. Due to the application of a single coated CEM, the water crossover was reduced by up to 54%.

The coating procedure, as well as the experimental procedures, are described in the following.

2. Experimental Section

2.1. Membrane Coating

Two types of CEMs were coated with an interfacial polymerization technique. The not reinforced CEM Fumasep FKE-50 with a thickness of 50 µm and the PEEK-reinforced CEM Fumasep FKB-PK-130/ED-100 with a thickness of 130 µm (Fumatech BWT GmbH) underwent the following coating procedure on one side. Before the coating procedure, the membrane sample was rinsed and soaked in deionized water for at least 24 h. Following this, the membrane was fixed in the frame of an in-house designed coating cell, which used an o-ring and a flat seal to seal the cell on the sides and enabled a clear one-sided coating of the membrane surface. A small coating cell was used to coat membrane samples of the FKE-50 CEM and a larger cell fitted the FKB-PK-130/ED-100 membranes. The designing of the coating cells is schematically depicted in **Figure 2**b.

The steps of the coating procedure are visualized in Figure 2a. First, 40 mL (10 mL for the smaller coating cell) of aqueous piperazine (>99%, Sigma-Aldrich) solution containing 2 wt% piperazine was applied on the membrane surface. After an exposure time of 1 h, the piperazine solution was removed, and the membrane surface was rinsed with 50 mL

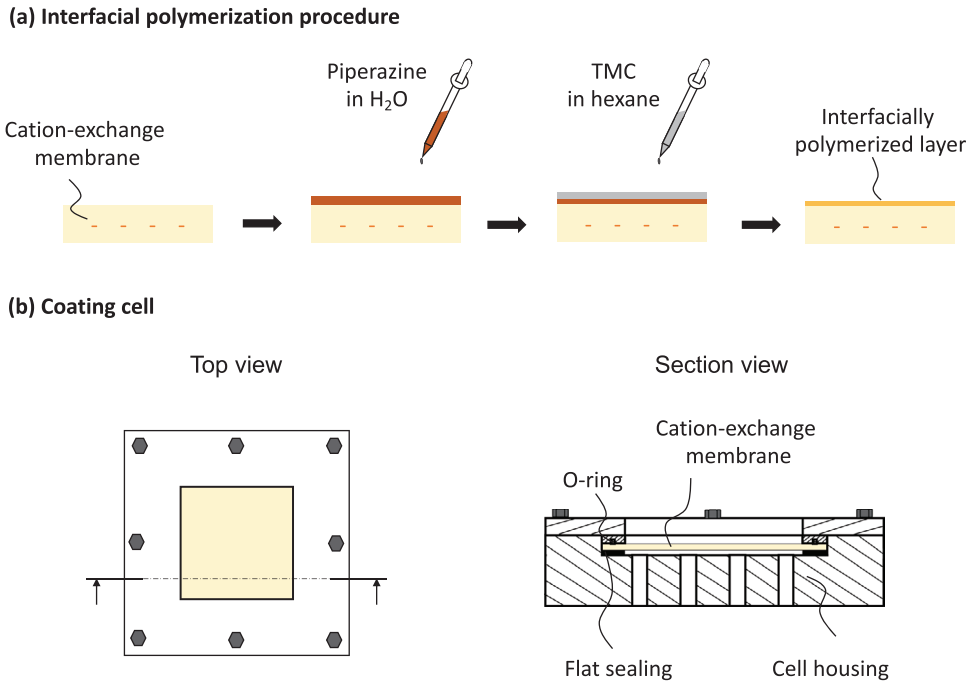

Figure 2. a) Schematic visualization of the coating procedure of a cation-exchange membrane (CEM) and b) drawing of the used coating cell in top view (left) and section view (right).

(12 mL) deionized water to remove excess piperazine. The membrane was dried in a fume hood for 30 min until no water drops remain on the membrane surface. As a next step, 40 mL (10 mL) of a 2 wt% solution of trimesoyl chloride (TMC, >98%, Sigma-Aldrich) in hexane (>99%, Carl Roth GmbH & Co. KG) was applied to the membrane. TMC and hexane were stored in a glove-box under a purified dry nitrogen atmosphere to prevent the reaction of TMC with air moisture. After an exposure time of 15 min, the solution was removed, and the membrane was rinsed with 50 mL (12 mL) pure hexane. After leaving the membrane in the fume hood for another 15 min, the remaining hexane was evaporated, and the membrane was removed from the coating cell. The coated membrane was then heated to a temperature of 40 °C in a convection oven and left overnight.

For imaging crosssections of the FKE-50 CEMs, samples were frozen and fractured in liquid nitrogen. FESEM images were taken with a Hitachi S-4800 scanning electron microscope.

2.2. Water Crossover in FCDI Experiments

All FCDI experiments presented in the following sections were performed using a continuous single module configuration, as described in the author previous publications.[8,14] The FCDI single module configuration was selected for this study, since it showed the greatest promise regarding cost- and energy-efficiency in our previous studies.[8,41]

The experiments were performed with an FCDI single module layout in AEM–CEM–AEM configuration. Since the aim of this study was to investigate and demonstrate the impact of the coating applied to the CEM on the water crossover through the membrane, the coated membrane was chosen to apply in the middle. In this location, the membrane was only in contact with the NaCl solutions and not the flow electrodes. This way, the investigation of cross-effects of the flow-electrodes on the water crossover could be avoided. Hence, the results were likely more comparable/transferable to other processes such as electrodialysis. Additionally, the impact of such a coating was likely highest in case of the center membranes, due to the highest concentration differences occurring across the central membrane. In the most extreme case, the membrane was the only separation between the diluate product stream (containing only a few g L^{-1} NaCl) and the concentrate product stream (containing >200 g L^{-1} NaCl).

The investigation of the impact of the module configuration on the water crossover and the impact of the membrane coating in case of other module configurations on the water crossover were relevant research questions for potential further studies.

Module Configuration: The FCDI cell applied in this study consisted of polyethylene endplates, flat gaskets, epoxy-impregnated graphite electrodes (Müller & Rössner GmbH & Co. KG, 180 × 180 × 10 mm) with flow channels for the flow electrodes (3 mm width, 2 mm depth, 200 cm overall length), one cation and two anion exchange membranes (Fumasep FKB-PK-130/ED-100 and Fumasep FAB-PK-130/ED-100, Fumatech BWT GmbH) with an effective surface area of 121 cm^2 and a 0.5 mm mesh spacer (Fumatech BWT GmbH, ED-100). Experiments were performed with 1) uncoated CEMs as reference experiments and 2) coated CEMs coated using the coating procedure described above. The cell was operated in cross-flow. The module layout is illustrated in **Figure 3**.

Before testing in the FCDI experiments all ion exchange membranes were soaked in the feed salt solutions, containing 60 or 120 g L^{-1} NaCl, for at least 24 h. Whenever an FCDI module was newly assembled, fixed amounts of water were recirculated separately through each flow electrode, diluate, and concentrate compartment for several hours to rule out internal and external leakages.

System Layout: The overall FCDI system layout is illustrated in **Figure 4**. The flow electrodes were recirculated through the FCDI systems using a peristaltic pump (Ismatec MCP process drive, Masterflex two-channel pump head Easy-Load II, Norprene tubing). The feed water was supplied by a second peristaltic pump (Ismatec Reglo ICC peristaltic pump with three independent channels). The electrical conductivity of the aqueous solutions was measured using conductivity sensors (LTC0,35/23; Sensortechnik Meinsberg). Two Keysight power supplies (Keysight Technologies Inc., E3466A) were applied,

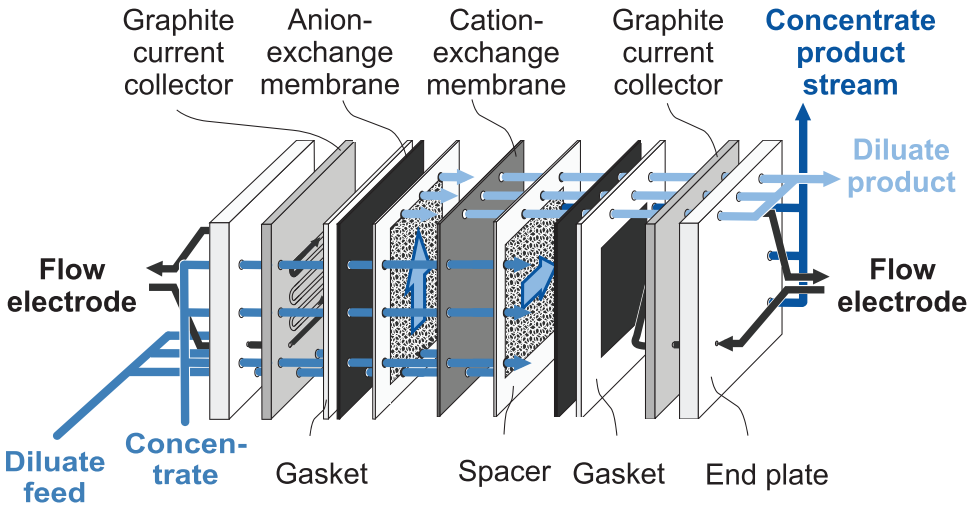

Figure 3. Illustration of the FCDI module layout applied for the water crossover experiments.

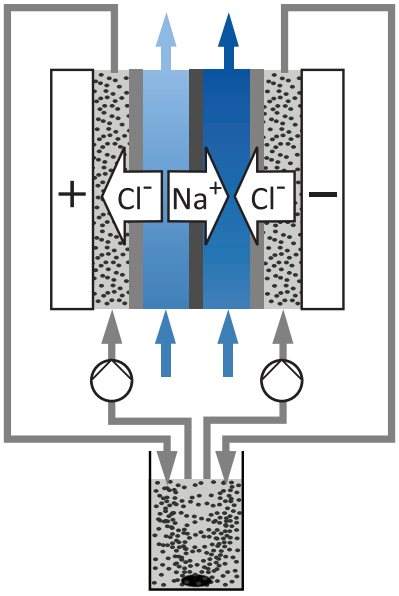

Figure 4. Illustration of the applied FCDI system layout including flow-electrode circuits. The crosslinked coating has been applied to the central membrane in the module (cation-exchange membrane).

and a digital multimeter (Voltcraft, VC270 Green-Line) was used to verify the actual voltage applied to the graphite current collectors. The pumps, power supplies, and conductivity sensors (LTC 0,35/23; Sensortechnik Meinsberg) were connected to a custom-made measuring system, "ZUMO-FUMS" (ZUMOLab GbR, Wesseling, Germany), which was used to control the pumps and power supplies as well as record the experimental data.

Table 1 gives an overview of the experimental settings. For each salt concentration, a reference experiment was performed with an uncoated membrane of the same base membrane material. All experiments described in this section were performed with activated carbon slurries used as flow electrodes prepared from 15 wt% Carbopal SC11PG (Donau Carbon GmbH) in a NaCl solution with a concentration equaling the feed concentration, either 60 or 120 g L^{-1} (sodium chloride ⩾99.8%, VWR Chemicals). The slurries were stirred overnight before use. For each flow-electrode circuit, the slurry was recirculated through the system at a flow rate of 150 mL min^{-1}. The slurry storage beakers were continuously stirred using magnetic stirrers. The feed flow rate for the diluate feed was set to 1 mL min^{-1}, and the feed flow rate for the concentrate feed was set to 0.04 mL min^{-1}. During steady-state operation, several diluate and concentrate stream samples were taken, and the density was measured to confirm the NaCl concentration.

Current–Voltage Characteristics: The current–voltage characteristics (*I–V* curves) of the different systems were investigated by a step-wise change of the applied voltage in a range between 0 and 2.5 V in steps of 0.1 V. After each change in voltage, the voltage was kept constant for 10 min, which corresponds to about two times the residence time. The steady-state electrical current was measured for each step.

During the measurements, the diluate feed flow rate was kept constant at 1 mL min^{-1}. To shorten the time until equilibrium is reached, the concentrate flow rate was kept at 1 mL min^{-1}.

3. Results and Discussion

3.1. Coating

We successfully applied the interfacial polymerization technique to the dense CEMs. Coating of the CEMs performed in the in-house coating cell results in a visible, slightly whitish polypiperazine-amide layer. In **Figure 5**a, a coated FKE-50 membrane sample is shown. The coated area of the membrane sample appears whitish compared to the uncoated edges of the sample. During the coating process, the aqueous solution containing the piperazine impregnates the membrane, and a piperazine layer is deposited on the surface of the membrane. Upon contact with the TMC from the hexane phase, piperazine is successfully crosslinked. The drying step before the contact to the TMC solution must be closely monitored. The remaining water drops on the membrane surface lead to a flaking layer. On the other hand, a well-dried membrane surface results in a well adhered polypiperazin-amide layer on the supporting CEM, which is defect-free by bare eye inspection. Figure 5b shows a FESEM image of the coated FKE-50 CEM. The typical "ridge-valley" morphology of polypiperazine-amide layer is visible, and the coating has an estimated thickness of around 500 nm approximated from the FESEM image. In contrast, the uncoated FKE-50 membrane has a smooth surface (cf. Figure 5c). The rough appearance of the CEM of the coated membrane sample is an artifact from the fracturing of the sample in liquid nitrogen, which is difficult to control. From the FESEM images, we conclude that the coating procedure successfully creates a crosslinked layer on the CEM.

For the Fumasep FKB-PK-130/ED-100, the coating procedure was scaled up and performed in the larger coating cell.

Table 1. Overview of parameter settings for desalination experiments.

Description	Cell Voltage [V]	Slurry NaCl [g L^{-1}]	Slurry Flow rate [mL min^{-1}]	Feed water NaCl [g L^{-1}]	Feed water Flow rate [mL min^{-1}]
Reference	1.2	60 and 120	150	60 and 120	Diluate:1/Concentrate:0.04
Modified CEM	1.2	60 and 120	150	60 and 120	Diluate:1/Concentrate:0.04

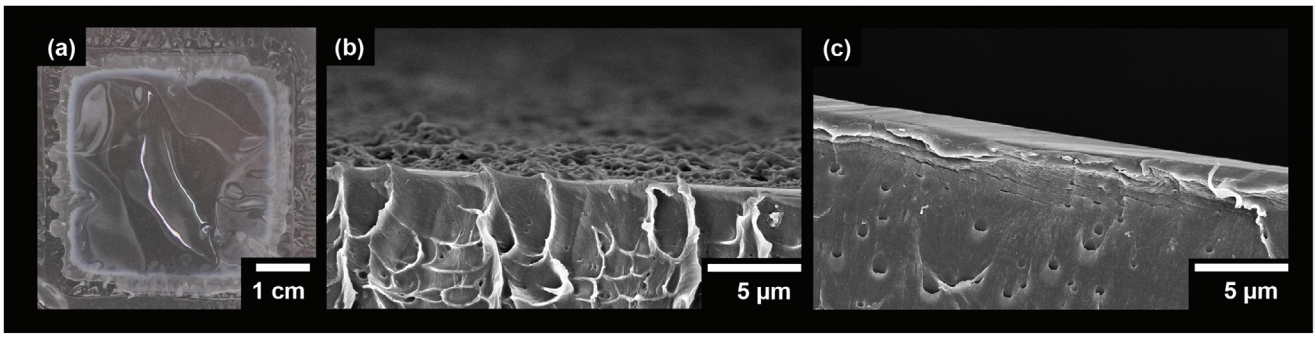

Figure 5. a) Top view of coated FKE-50 cation-exchange membrane, b) FESEM image of enlarged cross section of the coated surface of a FKE-50 cation-exchange membrane and c) enlarged FESEM image of the surface of a FKE-50 cation-exchange membrane.

The resulting layers are reproducible, scratch-proof, and easy to handle in the subsequent experiments.

3.2. Water Crossover in FCDI Experiments

In FCDI experiments, an FCDI cell's performance with an uncoated CEM was compared to the version of an FCDI cell with a CEM with a crosslinked coating, which was fabricated according to the above-described coating procedure. **Figure 6** shows the results of these FCDI experiments, which were performed in a single-module FCDI layout, as described above.

Figure 6a shows *I–V* curves measured at feed concentrations of 60 g L^{-1} NaCl and 120 g L^{-1} NaCl. While the coated membranes exhibit a nearly identical ohmic resistance, the main

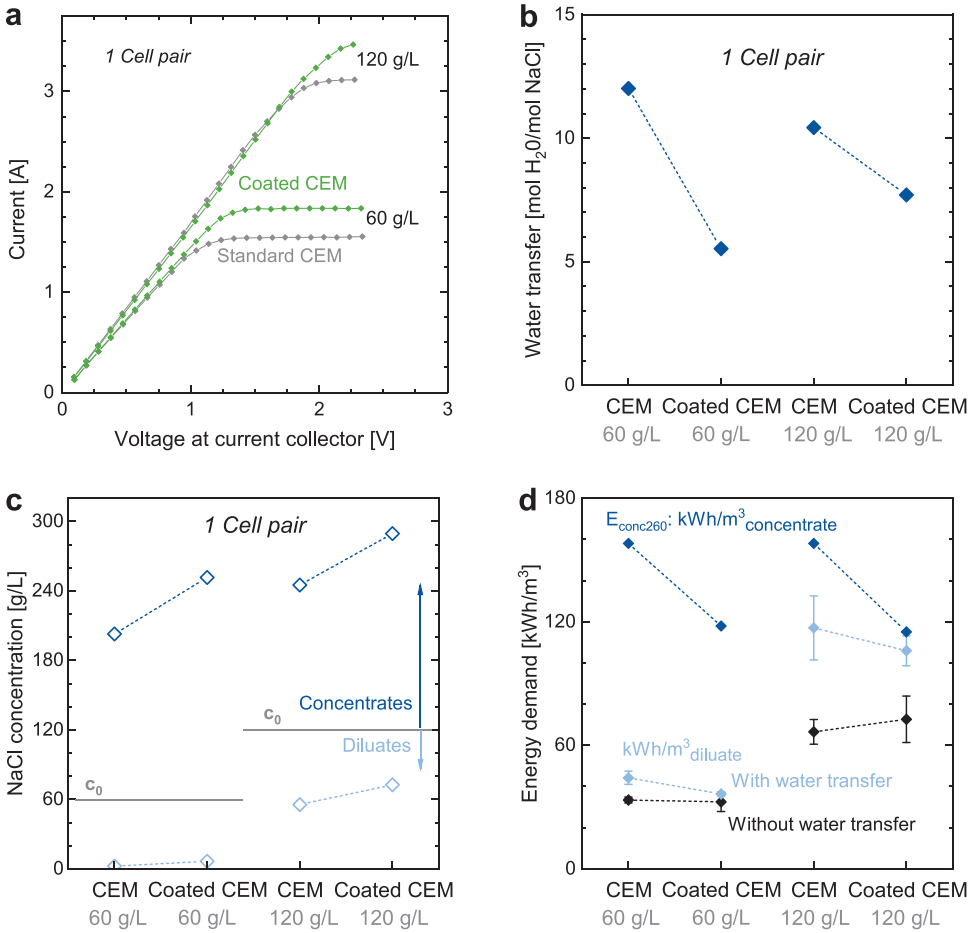

Figure 6. Results of desalination experiments with one cell pair at 60 and 120 g L^{-1} comparing modules assembled with the "standard" CEM to a module with a CEM with a crosslinked surface coating. a) *I–V* curves, b) water transfer in mole water per mole salt, c) NaCl concentrations of diluate and concentrate streams, and d) energy demand per m^3 product stream (for diluate with and without water transfer; normalized for full desalination to 0 g L^{-1} NaCl in case of diluates, and concentration up to 260 g L^{-1} NaCl in case of concentrates). Values do not account for pumping energy.

Table 2. Overview of results regarding the water and salt crossover in FCDI experiments.

	NaCl concentrations		Flow rates		
Diluate	Feed [g L^{-1}]	Diluate [g L^{-1}]	Feed diluate [mL min^{-1}]	Diluate [mL min^{-1}]	Salt transfer [g NaCl per min]
Reference	60	2.3	1	0.79	0.058
Modified CEM	60	6.5	1	0.99	0.054
Reference	120	55.4	1	0.73	0.079
Modified CEM	120	72.6	1	0.88	0.056
Concentrate	Feed [g L^{-1}]	Concentrate [g L^{-1}]	Feed concentrate [mL min^{-1}]	Concentrate [mL min^{-1}]	Water recovery [%]
Reference	60	202.9	0.04	0.28	74.2
Modified CEM	60	251.5	0.04	0.29	77.2
Reference	120	245	0.04	0.29	71.6
Modified CEM	120	289.5	0.04	0.28	75.7

difference between them seems to be the increased limiting current density. This result is surprising. Due to the addition of a coating layer, an increased ohmic resistance would seem likely. A reason for this could be the increased diluate concentration, as well as the increased concentrate concentration in the case of the experiments with coated membranes (cf. Figure 6c), which go hand in hand with reduced current efficiency. This may explain the increased limiting current, while the actual salt transfer stays similar. The reasons for this behavior become clearer when considering the other result figures, Figure 6b–d.

The results of desalination experiments are given in **Table 2** and plotted in Figure 6b–d show a reversed trend compared to the uncoated membranes. The surface coating use leads to a significant reduction in the water transfer rate and improved concentration performance. This is also visible in the reduced energy demand per cubic meter diluate and concentrate stream when considering the water transfer. The energy demand was calculated per volume of diluate or concentrate and normalized for full desalination to 0 g L^{-1} or concentration up to 260 g L^{-1}, respectively, to ensure a better comparability. The calculation was performed in the same way as described in our previous publication.[8]

As can be seen in Figure 6c and Table 2, the use of the CEM coated according to the coating procedure presented above leads to a simultaneous shift of the concentrations in the diluate and concentrate streams to higher concentrations. This was observed for both feed concentrations, 60 and 120 g L^{-1}.

This simultaneous shift of the concentrations in the diluate and concentrate streams is a contradiction at first glance. A possible explanation for this is the diluate flow rate: due to the more pronounced water transfer in case of the uncoated membranes, the diluate flow rate is reduced from 1 to 0.79 mL min^{-1} in case of an experiment with a 60 g L^{-1} feed solution, with a diluate concentration of 2.3 g L^{-1}. During the same investigation with a coated membrane, the diluate flow rate was only reduced to 0.99 mL min^{-1}, due to the reduced water transfer, while a diluate concentration of 6.5 g L^{-1} was achieved. The overall salt transfer rate from the diluate into the concentrate stream is comparable when using a coated CEM (0.054 g NaCl per min) compared to an uncoated CEM (0.058 g NaCl per min). A similar salt removal rate together with an increased diluate product flow rate, hence, leads to an increased diluate salt concentration measured at the outlet of the cell. In the case of the 120 g L^{-1} feed solution, this effect is even more pronounced, since in this case, the application of the coated membrane leads to a reduced salt transfer rate of 0.056 g NaCl per min (coated CEM) instead of 0.079 g NaCl per min (uncoated CEM).

In conclusion, the application of the additional crosslinked coating is a promising approach to improve the concentration performance of FCDI systems further while at the same time reducing the energy demand for concentration. Water transfer mainly leads to a dilution of the concentrate stream, making the membrane characteristics an essential factor for the successful application of FCDI for salt recovery and concentration, especially in high salinity conditions.

4. Conclusions

A crosslinked coating procedure for CEMs is presented in this work, reducing the water crossover in electrically-driven desalination and concentration processes applying ion-exchange membranes. The efficacy of the membrane coating is demonstrated using a FCDI process applied for desalination and concentration of saline brines at feed concentrations of 60 and 120 g L^{-1} NaCl. With the application of just a single coated CEM as a central membrane in the single-module FCDI cell, the water crossover was reduced by up to 54%.

The application of a CEM coated according to the coating procedure presented in this study leads to a significant improvement of the concentration performance due to a substantial reduction of the water transfer in the FCDI experiments performed in this study. Hence, the presented coating is promising for applying ion-exchange membrane processes aiming at the desalination and concentration of saline solutions, which especially suffer from pronounced water transfer.

In the future, the coating chemistry's effect on the water crossover can be further studied by changing the concentrations of the reactants or choosing different reactants for the coating. Moreover, investigating the shares of electroosmosis,

osmosis, and water drag related to ion transfer in the total water crossover, as well as the investigation of different module configurations on the water crossover, can give insight into future optimization potentials. Additionally, the impact of a comparable cross-linked coating on anion-exchange membranes on the water crossover could be studied.

Acknowledgements

A.R. and H.R. contributed equally to this work. This work was supported by the German Federal Ministry of Education and Research (BMBF) under the project "ElektroWirbel" (FKZ 13XP5008), BMBF-MOST "SepIon" (FKZ 02WIL1390), and by the European Research Council (ERC) under the European Unions Horizon 2020 research and innovation program (694946). This work was performed in part at the Center for Chemical Polymer Technology CPT, which is supported by the EU and the federal state of North Rhine-Westphalia (grant no. EFRE 30 00 883 02). M.W. appreciates the funding from the Alexander von Humboldt Foundation. The authors thank Karin Faensen for the high quality SEM images and Nils Weber, Nora Heinrich, Nora Grütering, Janna Kollbach, and Lynn Meyer for the preliminary work for this study.

Open access funding enabled and organized by Projekt DEAL.

Conflict of Interest

The authors declare no conflict of interest.

Data Availability Statement

Research data are not shared.

Keywords

brine concentration, flow-electrode capacitive deionization, ion-exchange membranes, selective coating, water desalination

Received: February 19, 2021
Revised: May 28, 2021
Published online: June 23, 2021

[1] *UN World Water Development Report 2019: Leaving No One Behind*, UNESCO, **2019**, oCLC: 1124775818.
[2] Environmental Management (Eds: V. Muralikrishna, V. Manickam), Butterworth-Heinemann, Oxford **2017**, ch. 12, pp. 249–293.
[3] M. Elimelech, W. A. Phillip, *Science* **2011**, *333*, 712.
[4] M. Suss, S. Porada, X. Sun, P. Biesheuvel, J. Yoon, V. Presser, *Energy Environ. Sci.* **2015**, *8*, 2296.
[5] S. Porada, R. Zhao, A. van der Wal, V. Presser, P. M. Biesheuvel, *Prog. Mater. Sci.* **2013**, *58*, 1388.
[6] Y. Li, T. Zhao, W. Yang, *Int. J. Hydrogen Energy* **2010**, *35*, 5656.
[7] T. Rottiers, K. Ghyselbrecht, B. Meesschaert, B. van der Bruggen, L. Pinoy, *Chem. Eng. Sci.* **2014**, *113*, 95.
[8] A. Rommerskirchen, C. J. Linnartz, F. Egidi, S. Kendir, M. Wessling, *Desalination* **2020**, *490*, 114453.
[9] A. Rommerskirchen, M. Alders, F. Wiesner, C. J. Linnartz, A. Kalde, M. Wessling, *J. Membr. Sci.* **2020**, *616*, 118614.
[10] W. Dai, H. Wang, X.-Z. Yuan, J. J. Martin, D. Yang, J. Qiao, J. Ma, *Int. J. Hydrogen Energy* **2009**, *34*, 9461.
[11] M. A. Anderson, A. L. Cudero, J. Palma, *Electrochim. Acta* **2010**, *55*, 3845.
[12] K. G. Nayar, P. Sundararaman, C. L. O'Connor, J. D. Schacherl, M. L. Heath, M. O. Gabriel, S. R. Shah, N. C. Wright, V. A. G. Winter, *Dev. Eng.* **2017**, *2*, 38.
[13] J. S. Tronc, F. Lamarche, J. Makhlouf, *J. Food Sci.* **1997**, *62*, 75.
[14] A. Rommerskirchen, Y. Gendel, M. Wessling, *Electrochem. Commun.* **2015**, *60*, 34.
[15] S. I. Jeon, H. R. Park, J. G. Yeo, S. Yang, C. H. Cho, M. H. Han, D. K. Kim, *Energy Environ. Sci.* **2013**, *6*, 1471.
[16] M. E. Suss, S. Porada, X. Sun, P. M. Biesheuvel, J. Yoon, V. Presser, *Energy Environ. Sci.* **2015**, *8*, 2296.
[17] P. Nativ, Y. Badash, Y. Gendel, *Electrochem. Commun.* **2017**, *76*, 24.
[18] Y. M. Volfkovich, *Russ. J. Electrochem.* **2020**, *56*, 18.
[19] C. Linnartz, A. Rommerskirchen, M. Wessling, Y. Gendel, *ACS Sustainable Chem. Eng.* **2017**, *5*, 3906.
[20] A. Rommerskirchen, B. Ohs, K. A. Hepp, R. Femmer, M. Wessling, *J. Membr. Sci.* **2018**, *546*, 188.
[21] A. H. Galama, M. Saakes, H. Bruning, H. Rijnaarts, J. W. Post, *Desalination* **2014**, *342*, 61.
[22] J. Kamcev, B. D. Freeman, *Annu. Rev. Chem. Biomol. Eng.* **2016**, *7*, 111.
[23] R. S. Kingsbury, S. Zhu, S. Flotron, O. Coronell, *ACS Appl. Mater. Interfaces* **2018**, *10*, 39745.
[24] Y. Tanaka, *Ion Exchange Membranes*, Elsevier, New York **2015**, pp. 87–99.
[25] K. P. Lee, T. C. Arnot, D. Mattia, *J. Membr. Sci.* **2011**, *370*, 1.
[26] J. E. Cadotte, R. S. King, R. J. Majerle, R. J. Petersen, *J. Macromol. Sci., Part A: Pure Appl. Chem.* **1981**, *A15*, 727.
[27] M. Paul, S. D. Jons, *Polymer* **2016**, *103*, 417.
[28] V. Freger, *Environ. Sci. Technol.* **2004**, *38*, 3168.
[29] X. Zhou, Z. Wang, R. Epsztein, C. Zhan, W. Li, J. D. Fortner, T. A. Pham, J. H. Kim, M. Elimelech, *Sci. Adv.* **2020**, *6*, eabd9045.
[30] A. Szymczyk, P. Fievet, *J. Membr. Sci.* **2005**, *252*, 77.
[31] A. Razmjou, M. Asadnia, E. Hosseini, A. Habibnejad Korayem, V. Chen, *Nat. Commun.* **2019**, *10*, 5793.
[32] B. Tansel, *Sep. Purif. Technol.* **2012**, *86*, 119.
[33] L. A. Richards, A. I. Schäfer, B. S. Richards, B. Corry, *Small* **2012**, *8*, 1701.
[34] R. Epsztein, E. Shaulsky, M. Qin, M. Elimelech, *J. Membr. Sci.* **2019**, *580*, 316.
[35] P. Nativ, O. Lahav, Y. Gendel, *Desalination* **2018**, *425*, 123.
[36] T. Luo, S. Abdu, M. Wessling, *J. Membr. Sci.* **2018**, *555*, 429.
[37] T. Luo, F. Roghmans, M. Wessling, *J. Membr. Sci.* **2020**, *597*, 117645.
[38] Khoiruddin, D. Ariono, Subagjo, I. G. Wenten, *J. Appl. Polym. Sci.* **2017**, *134*, 45540.
[39] F. Roghmans, E. Evdochenko, F. Stockmeier, S. Schneider, A. Smailji, R. Tiwari, A. Mikosch, E. Karatay, A. Kühne, A. Walther, A. Mani, M. Wessling, *Adv. Mater. Interfaces* **2019**, *6*, 1801309.
[40] W. Wang, R. Liu, M. Tan, H. Sun, Q. J. Niu, T. Xu, V. Nikonenko, Y. Zhang, *J. Membr. Sci.* **2019**, *582*, 236.
[41] A. Rommerskirchen, C. J. Linnartz, D. Müller, L. K. Willenberg, M. Wessling, *ACS Sustainable Chem. Eng.* **2018**, *6*, 13007.